American Mineralogist, Volume 69, pages 1173–1179, 1984

Roeblingite, $Pb_2Ca_6(SO_4)_2(OH)_2(H_2O)_4[Mn(Si_3O_9)_2]$: its crystal structure and comments on the lone pair effect

PAUL BRIAN MOORE

Department of the Geophysical Sciences
The University of Chicago
Chicago, Illinois 60637

AND JINCHUAN SHEN

X-ray Laboratory, Graduate School
Wuhan College of Geology
Beijing, China

Abstract

Roeblingite, $Pb_2Ca_6(SO_4)_2(OH)_2(H_2O)_4[Mn(Si_3O_9)_2]$, monoclinic holosymmetric, a = 13.208(4), b = 8.287(2), c = 13.089(9)Å, β = 106.65(6)°, space group $C2/m$, possesses a $^2_\infty[Mn(Si_3O_9)_2]^{10-}$ corner-linked sheet oriented parallel to $c\{001\}$, the plane of perfect micaceous cleavage. R = 0.066 for 2479 nonequivalent reflections.

The large cations are tucked between the $[Mn(Si_3O_9)_2]$ sheets. All vertices of the MnO_6 octahedron link to the (Si_3O_9) radicals which are oligosilicate three-membered rings and are geometrically similar to the rings in paragenetically related margarosanite, $PbCa_2[Si_3O_9]$. Coordination polyhedra include $Pb\phi_7$ (maximal point symmetry $mm2$); $Ca(1)\phi_8$ distorted square antiprisms; $Ca(2)\phi_7$ polyhedra similar to $Pb\phi_7$; MnO_6 octahedra; SiO_4, SO_4 tetrahedra. Mean bond distances are: Pb–O 2.82 (2.22 to 3.42), Ca(1)–O 2.53, Ca(2)–O 2.43, Mn–O 2.22, Si(1)–O 1.64, Si(2)–O 1.62 and S–O 1.47Å.

The packing efficiency, defined as the volume of the unit cell divided by the total number of anions in that cell, is usually close to the values of hcp or ccp oxysalt structures for most minerals which don't have channels. This value, V_E, is unusually large for Pb(II) oxysalts. By including the number of lone pair cations for that cell, the value, V_{E+L}, is more reasonable and approximates the packing efficiencies for oxysalts with those cations of similar size but stripped of all valence electrons.

Introduction

Roeblingite is an exotic phase, presently known from two localities. It was described from the type locality at Franklin, New Jersey (Penfield and Foote, 1897) as a *sulfite*-bearing silicate; Blix (1931) showed that it is a *sulfate*-bearing silicate, based on the Franklin material and a more recent find from Långban, Sweden where it occurred as fracture fillings. Foit (1966) examined its crystallographic character on coarse platy Långban material. We agree with his findings, except that the space group appears to be $C2/m$, not $C2/c$. Finally, Dunn et al. (1982) reported several new chemical analyses on roeblingite, but the differences from the Blix analysis are small. We include their chemical analysis for a Långban roeblingite in Table 1.

The senior author has long been interested in roeblingite; over fifteen years ago, crystals were secured from the Swedish Natural History Museum with plans of eventually unravelling its structure, and especially determining the role of the sulfur cation. More recently, increased interest in Pb(II) from oxysalt and sulfosalt environments and the micaceous nature of the material prompted a more detailed structure investigation.

Experimental procedure

At least ten chemical analyses have been reported in the literature, and three are selected for Table 1. One of the motivations for the present study concerns the formal charge on sulfur: is it S^{4+} or S^{6+}? Penfield and Foote (1897) were cautious in their study and reported SO_2 as the oxide. However, Blix (1931) re-investigated the problem, analyzing Franklin material and the recent find of Långban material. He concluded that sulfur occurred as SO_3, a conclusion we similarly make on the basis of structure study, for Långban material at least.

A small vial of palest pink flakes from Långban,

0003–004X/84/1112–1173$02.00

Table 1. Roeblingite: selected chemical analyses

	1	2	3	4
K_2O	0.13	-	-	-
Na_2O	0.40	-	-	-
PbO	31.03	30.04	30.7	30.48
SrO	1.40	2.79	0.7	-
MnO	2.48	2.49	4.4	4.84
CaO	25.95	23.12	22.6	22.97
SO_2	9.00	-	-	-
SiO_2	23.58	23.57	24.6	24.63
CO_2	-	0.61	-	-
SO_3	-	10.81	10.6	10.93
H_2O	6.35	6.60	[6.13]	6.15
Total	100.32	100.03	99.73	100.00

[1]Penfield and Foote (1897). Franklin, N.J.

[2]Blix (1931). Franklin, N.J.

[3]Dunn et al. (1982). A Smithsonian specimen, labelled NMNH B17051. Långban, Sweden.

[4]Calculated for $Pb_2Ca_6(SO_4)_2(OH)_2(H_2O)_4[Mn(Si_3O_9)_2]$.

Sweden was obtained from the Swedish Natural History Museum. It came from a large specimen showing a thick transverse fracture filled with roeblingite. Unfortunately, the exact specimen number was lost although it came from the same drawer which housed the material analyzed by Blix.

Clear plates were selected but considerable difficulty was encountered in obtaining a suitable single crystal as the surfaces are usually crinkled. One thin platy clear pale pink fragment was secured which measured 197 mμ ($\|a$) × 100 mμ ($\|b$) × 25 mμ ($\|c$). The crystal shape was approximated by indexed faces after the corners and edges were measured on a two-circle goniometer fitted with a micrometer ocular. Assorted precession photographs demonstrated the satisfactory quality of the reflections and provided initial unit cell parameters. Extinctions suggested $C2$, Cm or $C2/m$, the last space group supported by success of the refinement. The crystal was transferred to a Picker FACS-1 automated diffractometer with graphite monochromator and Mo$K\alpha$-radiation (λ = 0.70926Å). Prior to complete data collection, the cell parameters were refined, giving a = 13.208(4), b = 8.287(2), c = 13.089(9)Å, β = 106.65(6)°, space group $C2/m$ (*vide infra*). With scan speed 2° min^{-1}, base scan width of 2°, background counting times of 20 sec on each side of the peak, a total of 3267 reflections was collected to 2θ = 70° ($\sin\theta/\lambda$ = 0.81). After Lorentz-polarization correction, the data were merged by the AGNOST program using a calculated absorption coefficient μ = 135.5 cm^{-1}. The reliability of symmetry equivalent reflections, R_s = 0.049, indicated satisfactory quality of the data. A total of 2479 independent $|F_o|$ was available throughout the study; programs including SHELX-76, were run on the DEC VAX 11/780 computer facility at The University of Chicago.

Solution and refinement of the structure

Roeblingite's composition suggested an ideal "heavy atom" problem by first locating the Pb vectors on a $P(uvw)$ map, then identifying the other atoms X from the Pb–X vectors. The order of decreasing vector density would be Pb–Pb ≫ Pb–Ca > Pb–S > Pb–Si > Pb–O ≫ Ca–Ca. This proved to be an excellent strategy and all non-hydrogen atoms were easily located. The Pb atom resided on ($x0z$), equipoint number 4, point symmetry m.

Table 2. Roeblingite: atomic coordinate and anisotropic thermal vibration (×10^3) parameters†

	x	y	z	U_{11}	U_{22}	U_{33}	U_{12}	U_{13}	U_{23}
Pb	0.1010(1)	0.0000	0.1450(1)	13.4(3)	11.5(3)	14.5(3)	0	3.0(2)	0
Mn	0.0000	0.5000	0.5000	10(2)	10(2)	16(2)	0	3(1)	0
Ca(1)	0.0549(3)	0.5000	0.2371(3)	12(1)	11(1)	15(1)	0	4(1)	0
Ca(2)	0.3042(2)	0.2306(3)	0.3307(2)	9(1)	9(1)	15(9)	2(1)		2(1)
Si(1)	0.2632(4)	0.5000	0.4846(4)	8(2)	7(2)	13(2)	0	3(1)	0
O(1)	0.2217(10)	0.5000	0.3592(10)	9(4)	18(6)	14(5)	0	5(4)	0
*O(2)	0.3224(10)	0.0000	0.4472(11)	6(5)	29(7)	22(6)	0	12(4)	0
O(3)	0.1552(7)	0.1580(10)	0.4802(7)	12(3)	5(3)	17(3)	-4(3)	3(3)	10(3)
Si(2)	0.0612(2)	0.1732(4)	0.3690(3)	8(1)	5(1)	15(1)	2(1)	4(1)	1(1)
O(4)	0.1173(7)	0.1938(12)	0.2742(7)	14(4)	17(4)	13(3)	-3(3)	8(3)	-7(3)
O(5)	0.4870(7)	0.1768(11)	0.3708(7)	12(3)	3(3)	23(4)	-4(3)	3(3)	-4(3)
O(6)	-0.0011(10)	0.0000	0.3571(12)	10(5)	2(4)	31(6)	0	11(4)	0
S	0.2626(4)	0.5000	0.1123(3)	15(2)	11(2)	14(2)	0	7(1)	0
O(7)	0.2851(13)	0.5000	0.0088(12)	29(7)	25(7)	20(6)	0	15(5)	0
O(8)	0.1475(13)	0.5000	0.1018(14)	22(7)	38(8)	26(7)	0	5(6)	0
O(9)	0.3101(9)	0.3581(13)	0.1728(9)	34(5)	16(4)	25(4)	10(4)	17(4)	8(4)
OW(1)	0.2754(10)	0.0000	0.2143(11)	9(5)	17(6)	16(5)	0	4(4)	0
OW(2)	0.4460(9)	0.1742(15)	0.0967(9)	19(4)	26(5)	30(5)	2(4)	1(4)	-2(4)

†Estimated standard errors refer to the last digit. The anisotropic thermal vibration parameters are coefficients in the expression $\exp-[U_{11}h^2 + U_{22}k^2 + U_{33}\ell^2 + 2U_{12}hk + 2U_{13}h\ell + U_{23}k\ell]$.

*Non-positive definite thermal parameter.

Successive Fourier electron density maps and difference syntheses revealed 18 non-equivalent atoms in the asymmetric unit. Special attention was devoted to the S atom. We concluded, for our crystal at least, that an $(SO_4)^{2-}$ tetrahedron was present and that the compound involved sulfate radicals.

Final refinement included 41 variable atomic coordinate parameters among the 18 non-equivalent atoms, 1 scale factor and 86 anisotropic thermal vibration parameters, giving a data to variable parameter ratio of 19.4:1. A final difference synthesis failed to display any major residues, including the hydrogen atoms; small residues did occur within 2Å of the Pb atom, probably series termination errors.

$R = 0.066$ for all 2479 independent reflections, where

$$R = \Sigma \frac{||F_o| - |F_c||}{\Sigma |F_o|}.$$

Atomic coordinate and anisotropic thermal vibration parameters are given in Table 2, structure factor tables in Table 3[1] and bond distances and angles in Table 4.

Description of the structure

Coordination polyhedra

As the structure involves several independent coordination polyhedra of intermediate size (C · N · = 6–8), the tabulation of Britton and Dunitz (1973) is handy. Si(1), Si(2) and S are each in tetrahedral coordination with respect to oxygens; and Mn is in octahedral coordination. Due to the $6s^2$ lone pair, the coordination polyhedron about Pb is considerably distorted, with Pb–O ranging from 2.22 to 3.42Å (Table 4). For Pb and for the other large cations, the cutoff was selected as the first cation–cation distance. In effect, the coordination numbers suggested by Table 4 are upper limits. For seven oxygens coordinating to Pb, the polyhedron approximates no. 23 in Britton and Dunitz, with maximal point symmetry $C2v$ ($mm2$). This polyhedron is especially common for 7-coordinate Ca^{2+}, and can be generated by fusing a square pyramid and a trigonal prism at a square face; it is also found for Ca(2)ϕ_7. The Ca(1)ϕ_8 is a distorted square antiprism, polyhedron no. 128 with maximal point symmetry $D4d$ ($\bar{8}2m$).

Bond distances

Roeblingite poses a few small challenges for the crystal chemist. The larger-sized cations (Ca(II) and Pb(II)) require careful selection of coordination number. For calcium we accepted all bonds up to the first cation–cation distance; the same holds for Pb(II), except that the lone pair distorts the polyhedron substantially. The mean polyhedral distances (with coordination numbers as superscripts) are $^{[7]}$Pb–O 2.82 (2.22 to 3.42), $^{[8]}$Ca(1)–O 2.53, $^{[7]}$Ca(2)–O 2.43, $^{[6]}$Mn–O 2.22, $^{[4]}$Si(1)–O 1.64, $^{[4]}$Si(2)–O 1.62 and $^{[4]}$S–O 1.47Å, the last coincident with the average of three $^{[4]}$S–O 1.47Å in α-$Fe_2(SO_4)_3$ (Moore and Araki, 1974).

Structural principles

Locally abundant, brittle micaceous platy masses of roeblingite from Långban suggested a structure possibly allied to the brittle micas. Thus, Moore (1971) proposed the formula $Pb_2Ca_7[Si_2O_5]_3[SO_4]_2(OH)_8$ for the mineral. Dunn et al. (1982) proposed for Z = 2, $(Ca,Sr)_6(Mn,Ca)Pb_2(SO_4)_2(Si_6O_{14})(OH)_{10}$ but the crystal structure was not yet known. Therefore, it was a surprise that structure analysis demonstrated an arrangement based on oligosilicate trimers, the 3-ring $[Si_3O_9]^{6-}$, geometrically allied to the paragenetically related phase, margarosanite, $PbCa_2[Si_3O_9]$ (Freed and Peacor, 1969). Again, we note that a structural formula proposed in advance of knowledge of the crystal structure can often be wrong.

It is possible to write a formula displaying the roebling-

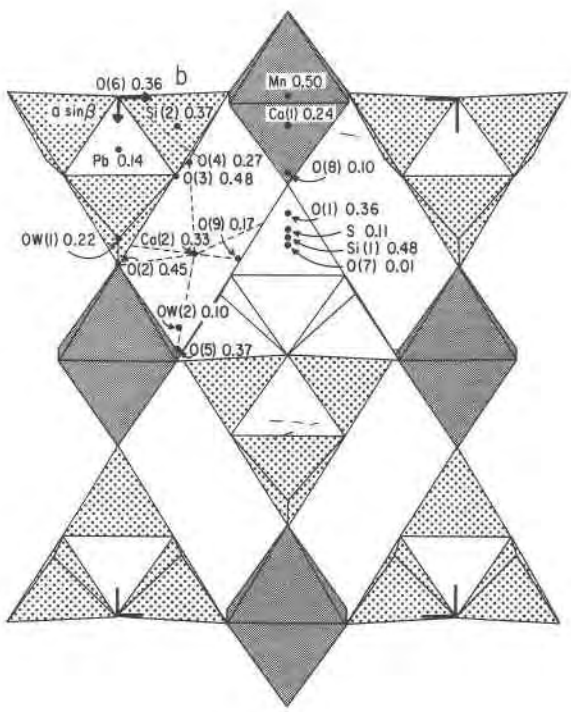

Fig. 1. Polyhedral diagram with labelled asymmetric unit for roeblingite projected down [001]. The MnO_6 octahedra are finely stippled and the $[Si_3O_9]$ 3-rings are coarsely stippled. Note some $[Si_3O_9]$ related by inversion at (000) have been omitted, and one $[Si_3O_9]$ at (½½0) is not stippled. This attempts to emphasize the $^2_\infty[Mn(Si_3O_9)_2]$ fbb, the reason for micaceous cleavage on {001}.

[1] To obtain a copy of Table 3, order Document AM-84-254 from the Business Office, Mineralogical Society of America, 2000 Florida Avenue, N.W., Washington, D.C. 20009. Please remit $5.00 in advance for the microfiche.

Table 4. Roeblingite: bond distances and angles†

Mn		**S**		
4 Mn-O(5)$^{(1)}$	2.21(1)	2 S-O(9)	1.46(1)	
2 -O(2)$^{(1)}$	2.25(1)	1 -O(7)	1.47(1)	
average	2.22 Å	1 -O(8)	1.49(2)	
		average	1.47	
2 O(5)-O(5)$^{(3)}$	2.93(2)	[1 S-O(1)	3.43(1)]	
4 O(2)-O(5)	3.02(2)	[2 S-Ca(2)	3.543(6)]	
4 O(2)$^{(5)}$-O(5)	3.28(2)			
2 O(5)-O(5)$^{(6)}$	3.30(2)	1 O(9)-O(9)$^{(3)}$	2.35(2)	107.8(10)
average	3.14	2 O(7)-O(9)	2.39(2)	109.4(5)
		2 O(8)-O(9)	2.39(2)	108.7(6)
Pb		1 O(7)-O(8)	2.46(2)	112.8(9)
1 Pb-OW(1)	2.22(1)	average	2.39	109.5
2 -O(4)	2.30(1)			
1 -O(7)$^{(1)}$	2.84(1)	**Si(1)**		
2 -OW(2)$^{(1)}$	3.34(1)	1 Si(1)-O(1)	1.57(1) Å	
1 -O(6)	3.42(1)	1 -O(2)$^{(1)}$	1.63(1)	
average	2.82	2 -O(3)$^{(1)}$	1.67(1)	
[2 Pb-Si(2)	3.437(4)]	average	1.64	
		[2 Si(1)-Si(2)$^{(1)}$	2.926(6)]	
Ca(1)				
1 Ca(1)-O(1)	2.32(1)	2 O(1)-O(3)$^{(1)}$	2.61(2)	
1 -O(8)	2.42(2)	1 O(3)$^{(1)}$-O(3)$^{(4)}$	2.62(2)	
2 -OW(2)$^{(2)}$	2.45(1)	2 O(2)$^{(1)}$-O(3)$^{(1)}$	2.71(2)	
2 -O(5)$^{(2)}$	2.63(1)	1 O(1)-O(2)$^{(1)}$	2.76(2)	
2 -O(4)	2.67(1)	average	2.67	
average	2.53			
[2 Ca(1)-Si(2)	3.200(4)]	**Si(2)**		
		Si(2)-O(5)$^{(2)}$	1.59(1)	
Ca(2)		-O(3)	1.63(1)	
Ca(2)-O(9)	2.34(1)	-O(4)	1.63(1)	
-O(5)	2.36(1)	-O(6)	1.64(1)	
-O(4)	2.39(1)	average	1.62	
-OW(1)	2.40(1)	[1 Si(2)-Si(2)$^{(3)}$	2.871(6)	
-O(2)	2.41(1)			
-O(3)$^{(1)}$	2.55(1)	O(3)-O(6)	2.58(2)	104.5(6)
-O(1)	2.56(1)	O(3)-O(4)	2.61(2)	107.1(5)
average	2.43	O(4)-O(5)$^{(2)}$	2.64(2)	110.3(6)
[Ca(2)-Si(1)	3.156(4)]	O(3)-O(5)$^{(2)}$	2.65(2)	111.3(6)
		O(4)-O(6)	2.68(2)	110.2(6)
		O(5)$^{(2)}$-O(6)	2.69(2)	113.0(6)
		average	2.64	109.4

†Estimated standard errors in parentheses refer to the last digit. The equivalent positions (referred to Table 2) are designated as superscripts and are (1) = ½-x, ½-y, -z; (2) = ½+x, ½-y, z; (3) = x, -y, z; (4) = ½-x, ½+y, -z; (5) = ½+x, ½+y, z; (6) = -x, y, -z.

ite–margarosanite relationship:

$$\underset{\text{roeblingite}}{Pb_2Ca_6(SO_4)_2(OH)_2(H_2O)_4[Mn(Si_3O_9)_2]} \rightarrow$$

$$\underset{\text{margarosanite}}{2PbCa_2[Si_3O_9]} + \underset{\text{hypothetical}}{Ca_2Mn[SO_4]_2(OH)_2(H_2O)_4}.$$

But this does not correctly portray the structural principle. Rather, an infinitely extending planar trellis $^{2}_{\infty}[Mn(II)(Si_3O_9)_2]^{10-}$ forms the basis of the structure. This sheet-like design is parallel to {001} where the individual $[SiO_4]$ tetrahedra and $[MnO_6]$ octahedra are corner-linked to each other, forming the most rigid planar component in the structure. Figure 1 is a polyhedral diagram of the structure down [001]. In fact bonds, other than O–H...O,

which penetrate the {001} plane, include ...Pb–O(7)–S–O(9)–Ca(2)... and ...Ca(1)–O(8)–S... , the $[SO_4]$ insular unit acting as a bridge between $[Mn(Si_3O_9)_2]$ parallel to {001}. These bonds, which involve the large Ca(1), Ca(2) and Pb cations, have lower bond strength than Si–O–Si and Si–O–Mn linkages and probably explain the brittle, rather than flexible, physical properties of the compound. Figure 2 portrays a projection of the structure down [010] and aids in visualizing the perfect {001} cleavage for the mineral.

A most interesting point is the relationship between regions of the roeblingite and margarosanite structures. These phases formed under similar conditions, in a paragenesis which is closely related if not connected, at least at Franklin, New Jersey (Palache, 1937, p. 70, 113). The fundamental $[Si_3O_9]$ units in roeblingite and margarosanite are featured in Figure 3. In both structures, the geometrical similarities of the $[Si_3O_9]$ rings are striking. Moreover, a weaker but still pronounced disposition of the Ca(2) atoms in roeblingite and the Ca(2) and Ca(1) atoms in margarosanite can be noted. Beyond this, there is no further structural similarity between the remaining regions in roeblingite and in margarosanite.

Emphasis has been placed on the similar $[Si_3O_9]$ geometry in both structures because it displays yet again a close structural similarity between paragenetically related phases, and suggests that certain clusters may be confined to particular regions in P, T, X space as suggested by Hawthorne (1979) for a particular cluster which repeatedly occurs in hydrothermal and secondary pegmatite phosphate assemblages. If this is indeed the link between crystal structure and paragenesis, then crystal structures of phases in a similar paragenesis should be scrutinized particularly carefully for these isomorphic

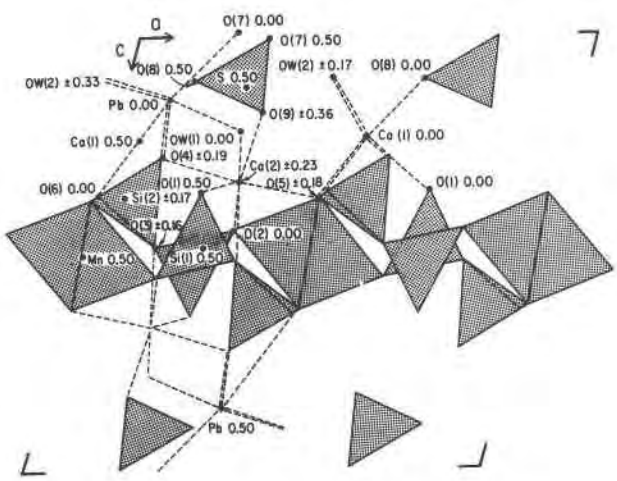

Fig. 2. Roeblingite polyhedral diagram down [010] with large cation bonds dashed in. The stippled $^2_\infty[Mn(Si_3O_9)_2]$ sheet appears prominently and the {001} cleavage plane breaks relatively few long (~2.4Å) bonds.

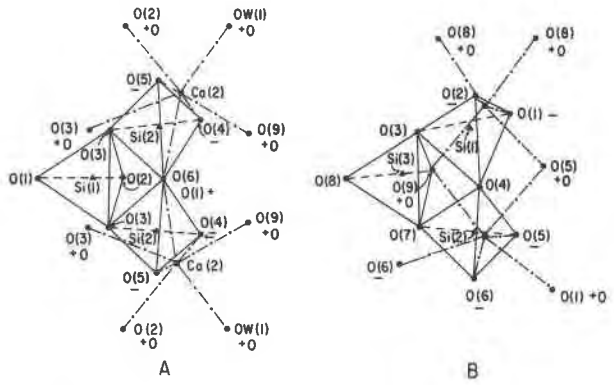

Fig. 3. Similar clusters in roeblingite (A) projected down [100] and margarosanite (B) projected down [100]. The Si(1)Si(2)$_2$O$_9$ rings and Ca(2), Ca(2) large cations in roeblingite; and Si(1)Si(2)Si(3)O$_9$ rings and Ca(2), Ca(1) large cations in margarosanite (squares) are partly isomorphic. Ca–O bonds are shown as dot–dash lines and relative heights of oxygens to bonded calcium are noted.

clusters or "fundamental building blocks." In addition, the aforementioned $^2_\infty[Mn(II)(Si_3O_9)_2]^{10-}$ sheet may serve as a fundamental building block for other species, but the present platy lead silicate structures are poorly understood and speculation on the unknown structures is premature.

Freed and Peacor (1969) noted that margarosanite can be considered a distortion of close-packing. In much the same fashion, it is possible to consider roeblingite as based on the {3^6} net in the (001) plane. Figure 4 is an idealization of Figure 1; the idealized atom positions are mapped on the {3^6} net, with x = m/6, y = n/6, z = p/8 where m, n, p = integers. This would correspond to a projection down [110] in the rocksalt arrangement. Even rows along [010] should have m = even number and would alternate with m = odd number. This does not hold in general, which means the arrangement is not *sensu stricto* a close-packing. However, the average density of atoms at a nodal point is 4 along the [001] repeat and the anion packing efficiency approximates dense-packing. Note that all oxygens and lead atoms occur on the nodes of the {3^6} net, the Mn atoms at the centers of octahedra and the Ca, Si and S atoms near the centers of the triangles. Deviations of the anion frame, in Å units, are given in Table 5. The two severe deviations, where the deviation is greater than the effective ionic radius for O^{2-} (r = 1.40Å), are O(7) and Pb; this suggests that $[SO_4]$ is not commensurate with efficient packing on {3^6} and that the Pb(II) cation exhibits distortion due to lone pair geometry. Indeed, Pb resides in a coordination polyhedron of oxygens of order 7. The OW(1) 2.22 and 2 O(4) 2.29Å are larger than Pb(IV)–O 2.14Å, the latter calculated from Shannon and Prewitt (1969) for $^{[6]}Pb(IV)^{[3]}O_2^{2-}$, but much smaller than that calculated for $^{[6]}Pb(II)^{[3]}O^{2-}$ where Pb–O 2.54Å. The remaining distances in roebling-

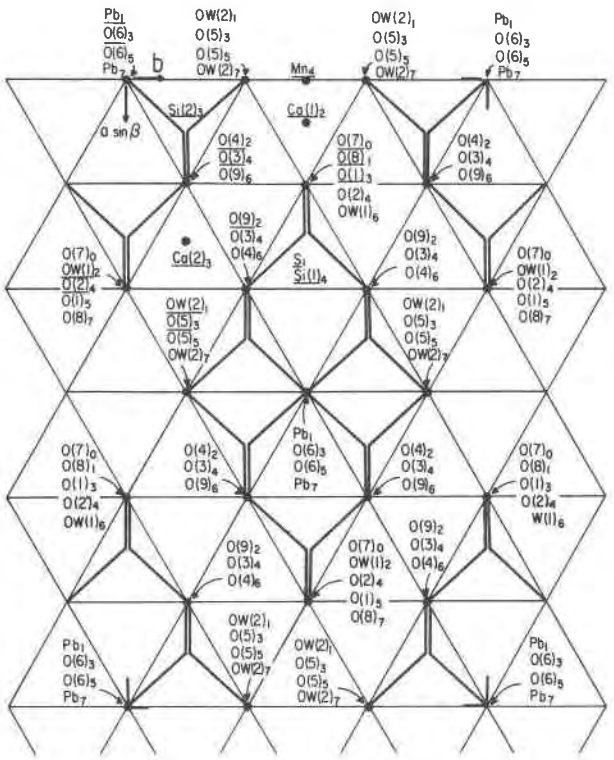

Fig. 4. Idealization of Figure 1, referred to the $\{3^6\}$ net. Atoms in the asymmetric unit are underlined. The fractional height z where $z = p/8$ is given as an integer in p.

ite range from Pb–O 2.83–3.43Å. From the shape of the polyhedron and the distances, the locus of the $6s^2$ lone-pair is inferred to be oriented toward the triangular O(6)–OW(2)–OW(2)′ face on the square pyramidal component of the $C2v$ polyhedron of order 7.

Lone pair geometry and packing efficiency

For a family of compounds as diverse and perplexing as oxysalts of Pb(II), it is desirable to seek a model in which they can be structurally related. As we have already seen, certain features of Pb(II) crystal chemistry in roeblingite appear rather unorthodox and inexplicable. First, in constructing the idealized model based on the $\{3^6\}$ net, Pb(II) was included in the anion frame on a nodal position. This is not in itself unusual. Large cations of elements with principal quantum number 6 approach O^{2-} in effective ionic radius, and often satisfy large coordination geometry through ordering over an anion site. For example in hibonite, $CaAl_{12}O_{19}$ or crystallographically written $Al_{12}O_{19}Ca$, the Ca atom occurs in the anion frame and is locally 12-coordinate by oxygens which define the vertices of a cuboctahedron (Kato and Saalfeld, 1968). Second, the $\{3^6\}$ net alone does not confer a close-packed (cubic, hexagonal or mixed sequences) structure as the close-packed layers are not necessarily planar with respect to the axis of projection.

Table 5. Ideal fractional coordinates for roeblingite, based on the $\{3^6\}$ net†

	Ideal					Ideal			
	x	y	z	Δ(Å)		x	y	z	Δ(Å)
O(1)	1/6	3/6	3/8	0.70	O(7)	1/6	3/6	0/8	1.60
O(2)	2/6	0	4/8	0.74	O(8)	1/6	3/6	1/8	0.46
O(3)	1/6	1/6	4/8	0.34	O(9)	2/6	2/6	2/8	1.15
O(4)	1/6	1/6	2/8	0.68	OW(1)	2/6	0	2/8	0.99
O(5)	3/6	1/6	3/8	0.19	OW(2)	3/6	1/6	1/8	0.88
O(6)	0	0	3/8	0.23	Pb	0	0	1/8	1.43

†x = m/6, y = n/6, z = p/8 where m, n, p are integers. The Δ is difference between ideal and real coordinates, multiplied by axial translations. Values which are greater than r = 1.40 Å (the oxide anion radius) are underlined.

Various nets, however, possess exceedingly efficiently packed structures, even though the structure types do not belong to the classical close-packings. For example, the $\{6^3\}$ and $\{(6 \cdot 3 \cdot 6 \cdot 3)^4\}$ hexagonal and Kagomé nets occur for the cation packings of the glaserite-derived structures (Moore, 1981). To assess the packing efficiency, the total number of anions in the unit cell was divided into the unit cell volume, and some packing efficiencies exceed the packing efficiency of an hcp or ccp polymorph by 10%. Paradoxically, although these structures were defined on the basis of the nets for the *cation* packings, the overall efficiency of packing was based on the number of *anions* in the unit cell. Exceedingly efficiently packed structures did not necessarily possess anion nets which could be referred to one of the classical close-packings.

Cations with a lone pair of electrons in the valence shell (such as Tl(I), Pb(II), Bi(III)) pose additional problems. Gillespie (1970) discusses in detail the polyhedral distortions which result due to a ns^2 lone pair of electrons in the valence shell of the central cation. Lone pair–lone pair, lone pair–bond pair and bond pair–bond pair interactions all contribute to distortion of the coordination polyhedron. One important question concerns the centroid of the lone pair of electrons with respect to the atom's nucleus, and the location of that centroid in space. The centroid of the lone pair was approximated from *ab initio* molecular orbital calculations for much lighter and isolated species such as OH_2, SH_3^+, NH_3, PH_3 by Schmiedekamp et al. (1979).

An alternative approach offered by Andersson and Åström (1972) is especially appealing to the crystal chemist. As the lone pair of electrons has a certain effective volume and distorts the neighborhood through lone pair–bond pair interactions, by counting up the total number of anions *and* lone pairs on the cations and dividing this into the cell volume, the effect of the lone pairs on the crystal structure could be assessed. This was done by comparing the calculated volume, V_{E+L}, with the total number of anions only divided into the cell volume, V_E. Taking pairs like the polymorphs of Pb(II)O and Pb(IV)O_2, they as-

Table 6. Packing efficiencies in assorted lead oxysalts†

Species	Formula	V_E, Å^3	V_{E+L}, Å^3
Paulmooreite	$Pb_2(As_2O_5)\psi_4$	31.06	17.26
Melanotekite	$Pb_2Fe_2O_2(Si_2O_7)\psi_2$	21.30	17.43
Queitite	$Pb_4Zn_2(SiO_4)(Si_2O_7)(SO_4)\psi_4$	23.98	18.93
Massicot	β-$PbO\psi$	38.18	19.09
Litharge	α-$PbO\psi$	39.20	19.60
Larsenite	$PbZn(SiO_4)\psi$	24.65	19.72
Margarosanite	$PbCa_2(Si_3O_9)\psi$	22.08	19.87
α-PbO_2	α-PbO_2	20.14	20.14
Roeblingite	$Pb_2Ca_6(SO_4)_2(OH)_2(H_2O)_4[Mn(Si_3O_9)_2]\psi_2$	21.45	20.18
Hyalotekite	ca. $Pb_2Ba_2Ca_2(B_2Be_4Si_{12}O_{28})F\psi_2$	22.04	20.62
Plattnerite	PbO_2	20.76	20.76

†V_E is the packing efficiency, or total anion cell contents divided into the unit cell volume. V_{E+L} is the packing efficiency, or total anion plus lone pair cation cell contents divided into the unit cell volume.

sessed the influence of the lone pair on unit cell volume and concluded that the lone pair effective volume approximated the volume of the O^{2-} anion.

We have done precisely this calculation in Table 6 for eleven Pb(II)-bearing oxysalts, including roeblingite. Cations in this table which possess lone pairs in the valence shell include Pb(II) and As(III). When the calculations are performed for volume per anion in the cell, the range is extensive: from 20.14Å^3 for α-PbO_2 to 39.20Å^3 for litharge, α-PbO, a range of (48.6%). Rewrite litharge as α-$PbO\psi$ where ψ symbolizes the lone pair of electrons on Pb(II) and now treat ψ as an anion. Including ψ in the calculations and computing volume per anion *plus* lone pairs, the range is much more narrow, from 17.3Å for $Pb(II)_2As(III)_2O_5\psi_4$ to 20.76Å^3 for plattnerite, $Pb(IV)O_2$, a range of (16.8%). This suggests that any calculations of anion packings in crystal structures must involve the contributions of lone pair electrons on cations, as well as the anions themselves.

We note that the volumes per anion plus lone pairs (Å^3) are comfortably in the range of packing efficiencies for intermediate-sized cations. For example, $^{[6]}Ca^{[3]}(OH)_2$, a = 3.59Å, c = 4.90Å, Z = 1, yields 27.3Å^3; and $^{[6]}Mn^{[6]}O$, a = 4.44Å, Z = 4, yields 21.9Å^3. The average cation radii in Table 6 are somewhat smaller than Ca(II) and Mn(II) in $Ca(OH)_2$ and MnO, again lending credence to the suggestion that Pb(II) and Mn(II) oxysalts—and sulfosalts—may indeed have a sensible structural taxonomy, providing that the lone pair cations are taken into account. Bond length–bond strength correlations are not offered as the role lone pair cations play in these relations is, as yet, not clearly understood.

Acknowledgments

P.B.M. appreciates the small vial of roeblingite plates which was personally gathered over fifteen years ago at the Natural History Museum, Section for Mineralogy, Stockholm, Sweden, and the financial support for the present study under the NSF EAR81-21193 grant. J.S. acknowledges the Ministry of Education, the Peoples Republic of China.

References

Andersson, S. and Åström, A. (1972) The stereochemistry of the inert pair in some solid oxides or oxide-fluorides of Sb^{3+}, Bi^{3+} and Pb^{2+}. National Bureau of Standards Special Publication 364 (Proceedings of 5th Materials Research Symposium), 3–14.

Blix, R. (1931) The chemical composition of roeblingite. American Mineralogist, 16, 455–460.

Britton, D. and Dunitz, J. D. (1973) A complete catalogue of polyhedra with eight or fewer vertices. Acta Crystallographica, A29, 362–371.

Dunn, P. J., Norberg, J. A. and Leavens, P. B. (1982) Roeblingite: new chemical data. Mineralogical Magazine, 46, 341–342.

Foit, F. F., Jr. (1966) New data on roeblingite. American Mineralogist, 51, 504–508.

Freed, R. L. and Peacor, D. R. (1969) Determination and refinement of the crystal structure of margarosanite, $PbCa_2Si_3O_9$. Zeitschrift für Kristallographie, 128, 213–228.

Gillespie, R. G. (1970) The electron-pair repulsion model for molecular geometry. Journal of Chemical Education, 47, 18–23.

Hawthorne, F. C. (1979) The crystal structure of morinite. Canadian Mineralogist, 17, 93–102.

Kato, K. and Saalfeld, H. (1968) Verfeinerung der Kristallstruktur von $CaO \cdot 6Al_2O_3$. Neues Jahrbuch für Mineralogie Abhandlungen, 109, 192–200.

Moore, P. B. (1971) Mineralogy and chemistry of Långban-type deposits in Bergslagan, Sweden. Mineralogical Record, 4, 1154–1172.

Moore, P. B. (1981) Complex crystal structures related to glaserite, $K_3Na[SO_4]_2$: evidence for very dense packings among oxysalts. Bulletin de la Société française de Minéralogie et de Cristallographie, 104, 536–547.

Moore, P. B. and Araki, T. (1974) Structural hierarchies among minerals containing octahedrally coordinating oxygen. III. The crystal structure of monoclinic ferric sulfate, $Fe_2[SO_4]_3$, and some intriguing topological questions. Neues Jahrbuch für Mineralogie Abhandlungen, 121, 208–228.

Palache, C. (1937) The minerals of Franklin and Sterling Hill, Sussex County, New Jersey. United States Geological Survey Professional Paper 180.

Penfield, S. L. and Foote, H. W. (1897) Über Röblingite, ein neues, schweflige Saure und Blei enthaltendes Silicat von Franklin Furnace, N. J. Zeitschrift für Kristallographie, 28, 578–580.

Schmiedekamp, A., Cruickshank, D. W. J. Skaarup, S., Hargittai, I. and Boggs, J. E. (1979) Investigation of the basis of the valence shell electron pair repulsion model by *ab initio* calculation of geometry variations in a series of tetrahedral and related molecules. Journal of the American Chemical Society, 101, 2002–2010.

Shannon, R. D. and Prewitt, C. T. (1969) Effective ionic radii in oxides and fluorides. Acta Crystallographica, B25, 925–946.

Manuscript received, December 12, 1983;
accepted for publication, June 20, 1984.